

Lawrence Berkeley National Laboratory

Lawrence Berkeley National Laboratory

Title

Toward fully self-consistent simulation of the interaction of E-Clouds and beams with WARP-POSINST

Permalink

<https://escholarship.org/uc/item/9zp34020>

Authors

D.P., Furman, M.A.; Celata, C.M.; Sonnad, K.; Venturini, M.; Cohen, R.H.; Friedman, A.; Grote,
LLNL

Publication Date

2007-04-09

Toward fully self-consistent simulation of the interaction of E-Clouds and beams with WARP-POSINST*

J.-L. Vay[†], M.A. Furman, C.M. Celata, K. Sonnad, M. Venturini
Lawrence Berkeley National Laboratory, Berkeley, California, USA

R. H. Cohen, A. Friedman, D.P. Grote
Lawrence Livermore National Laboratory, Livermore, California, USA

To predict the evolution of electron clouds and their effect on the beam, the high energy physics community has relied so far on the complementary use of “buildup” and “single/multi-bunch instability” reduced descriptions. The former describes the evolution of electron clouds at a given location in the ring, or “station,” under the influence of prescribed beams and external fields [1], while the latter (sometimes also referred as the “quasi-static” approximation [2]) follows the interaction between the beams and the electron clouds around the accelerator with prescribed initial distributions of electrons, assumed to be concentrated at a number of discrete “stations” around the ring. Examples of single bunch instability codes include HEADTAIL [3], QuickPIC [4, 5], and PEHTS [6].

By contrast, a fully self-consistent approach, in which both the electron cloud and beam distributions evolve simultaneously under their mutual influence without any restriction on their relative motion, is required for modeling the interaction of high-intensity beams with electron clouds for heavy-ion beam-driven fusion and warm-dense matter science. This community has relied on the use of Particle-In-Cell (PIC) methods through the development and use of the WARP-POSINST code suite [1, 7, 8]. The development of novel numerical techniques (including adaptive mesh refinement, and a new “drift-Lorentz” particle mover for tracking charged particles in magnetic fields using large time steps) has enabled the first application of WARP-POSINST to the fully self-consistent modeling of beams and electron clouds in high energy accelerators [9], albeit for only a few betatron oscillations. It was recently observed [10] that there exists a preferred frame of reference which minimizes the number of computer operations needed to simulate the interaction of relativistic objects. This opens the possibility of reducing the cost of fully self-consistent simulations for the interaction of ultra-relativistic beams with electron cloud by orders of magnitude. The computational cost of the fully self-consistent mode is then predicted to be comparable to that of the quasi-static mode, assuming that several stations per be-

atron period are needed.

During the workshop, there was some debate about the number of stations per betatron period that are needed when using the quasi-static mode. The argument was made that if there is less than one station per betatron period, then artificial resonances can be triggered and the resulting emittance growth provides an upper bound. The emittance growth thus obtained will fall either above or below the operational requirements of the machine. In the latter case, one can conclude that the electron effect that has been simulated is of no concern. However, if the emittance growth that was obtained is above the threshold, then the results become inconclusive, and simulations which resolve the betatron motion are then needed. In this case, according to [10], the fully self-consistent approach becomes an option. The aim of this paper is to investigate whether this option is indeed practical.

The original implementation of the WARP-POSINST quasi-static mode and results of its initial benchmarking against HEADTAIL are given in [11]. Since then, the quasi-static mode has been parallelized, and the ability to apply the effect of the beam space charge on the beam itself was added as an option. We have implemented two options for the advancement of the particle positions, namely using maps (similar to HEADTAIL, which we label QSM mode), or using a leapfrog mover (Boris mover, similar to QuickPic, which we label QSL mode). Using maps allows one to use time steps equal to - or larger than - the betatron oscillation period. In order to study the dependence of the predicted emittance growth in the QSM mode, as a function of the number of stations per turn (or per betatron oscillation), we performed a parametric scan for a simplified model of the LHC, setting the beam parameters as prescribed right after its injection into the ring (see Table 1). We assumed continuous focusing, and an initial offset of the beam in x and v_y of 10% of the initial RMS transverse size in x and of the initial thermal velocity spread in y , as a seed for a hose-like instability during the interaction of the beam with the background of electrons. The instability leads to emittance growth, which is the quantity that we have recorded after the beam has gone through one turn of the ring. With nominal horizontal and vertical tunes of 64.28 and 59.31, and assuming that one needs a minimum of two electron-cloud stations per betatron oscillation, one would then expect that the calculation might start to converge as the number of stations per turn reaches 120 ap-

*This work was supported under the auspices of the U.S DOE by Univ. of Calif., LBNL and LLNL under contracts DE-AC02-05CH11231 and W-7405-Eng-48, and by the U.S.-LHC Accelerator Research Program (LARP). This research used resources of the National Energy Research Scientific Computing Center, which is supported by the Office of Science of the U.S. Department of Energy under Contract No. DE-AC02-05CH11231.

[†]jlway@lbl.gov

proximately. The simulations parameters that were used to obtain the results presented below are summarized in Table 2. Results reported on Fig. 1 are from simulations using mesh refinement with 5 grid levels (the resolution increasing by a factor of 2 in each direction from one level to the next), while the results reported in Tables 3 and 4 are from simulations using a unique high-resolution grid.

Fig. 1 summarizes the fractional emittance growth after one turn of the LHC when the number of stations ranges from 10 to 3000, and for initial density of electrons of 10^{12}m^{-3} , 10^{13}m^{-3} and 10^{14}m^{-3} . Below the threshold of 120 stations per turn, the simulated emittance growth falls, for both the horizontal and vertical planes, in a range that is as wide as two to three orders of magnitude. The range of variation narrows when the number of stations rises above the estimated threshold, and eventually converges when the number is ten times the threshold value or more, i.e. when the betatron oscillations are well resolved. We also note that the results are consistent with the prediction that an upper bound of the emittance growth is obtained when there are fewer than two stations per betatron oscillation.

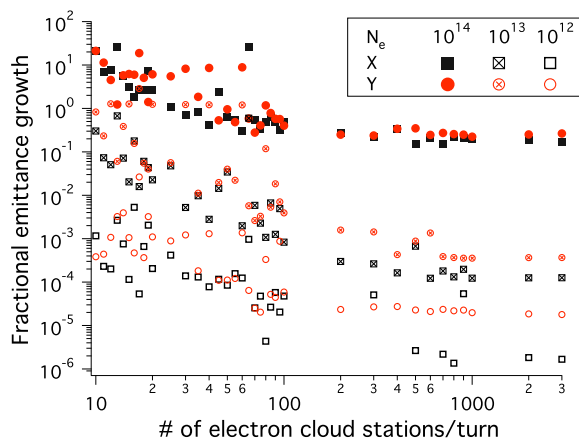


Figure 1: Fractional emittance growth versus number of electron-cloud stations per turn.

In Table 3 we contrast the fractional emittance growth after one turn between the QSM mode and the QSL mode, for initial electron densities ranging from 10^{10}m^{-3} to 10^{14}m^{-3} , in the case where the effect of the beam space charge on itself was turned off. The number of stations was set to 3000. We observe a fairly good agreement between the two modes for the highest value of the background density; however, for lower densities of electrons, the emittance growth levels to a higher value for the QSL than for the QSM. In Table 4, the results are presented for the QSM and QSL mode with the effect of the beam space charge on the beam itself turned on, and these are contrasted to the results from a fully self-consistent (FSC) run performed in a boosted frame of reference with $\gamma \approx 23$, chosen so that the number of time steps needed to push the beam through one turn is approximately 3000. The space-charge effect of the beam on itself alters substantially the QSM results for

low densities of electrons but not at larger densities, nor at any density for the QSL case. The QSL mode and the FSC modes agree very well for low densities of electrons. Since both the QSL and FSC mode utilize the same leapfrog particle pusher, this suggests that the leveling at low densities is related to the use of this pusher. At the highest densities, the emittance growth obtained in the horizontal (x) direction agree very well for all three modes. The QSM and QSL modes agree for the emittance growth in the vertical (y) direction, but the FSC mode predicts a somewhat higher value. For each mode, every run completed in a little more than one hour of CPU time using 32 processors of the NERSC supercomputer Bassi. This demonstrates that for a given number of stations chosen so that the betatron period is well resolved, a fully self-consistent simulation can model the interaction of a relativistic beam with a background of electrons for the same computational cost as that of the quasi-static approximation, provided that it is performed in the appropriate boosted frame of reference.

Further work is underway toward a full understanding of the differences in the results reported in Tables 3 and 4. This will be followed by an extension of the comparisons of the three modes to more detailed description of the lattice, and modeling the beam evolution for many turns.

REFERENCES

- [1] M. A. Furman and G. R. Lambertson, Proc. Intl. Workshop on Multibunch Instabilities in Future Electron and Positron Accelerators "MBI-97," KEK, p. 170; M. A. Furman, LBNL-41482/LHC Project Report 180, May 20, 1998. M. A. Furman and M. T. F. Pivi, PRST-AB 5, 124404 (2002)
- [2] P. Sprangle, E. Esarey, and A. Ting, *Phys. Rev. Letters* **64**, 2011-2014 (1990).
- [3] G. Rumolo and F. Zimmermann, *PRST-AB* **5** 121002 (2002).
- [4] C. Huang, V.K. Decyk, C. Ren, M. Zhou, W. Lu, W.B. Mori, J.H. Cooley, T.M. Antonsen, Jr. and T. Katsouleas, *J. of Comput. Phys.* **217**, 658-679 (2006).
- [5] G. Rumolo, A. Z. Ghalam, T. Katsouleas, C. K. Huang, V. K. Decyk, C. Ren, W. B. Mori, F. Zimmermann, and F. Ruggiero, *PRST-AB* **6** 081002 (2003).
- [6] K. Ohmi, 'Particle-In-Cell Simulation of Beam-Electron Cloud Interactions,' PAC 2001 Chicago, p. 1895 (2001).
- [7] D. P. Grote, A. Friedman, J.-L. Vay, I. Haber, AIP Conf. Proc. 749 (2005) 55.
- [8] J.-L. Vay, M. A. Furman, P. A. Seidl, R. H. Cohen, A. Friedman, D. P. Grote, M. Kireeff Covo, A. W. Molvik, P. H. Stoltz, S. Veitzer, J.P. Verboncoeur, *NIMPR A* **577**, 65-69 (2007)
- [9] Vay, J.-L.; Furman, M.; Cohen, R.; Friedman, A.; Grote, D., Proc. 21st Biennial Particle Accelerator Conference, PAC05, Knoxville, TN, (2005)
- [10] J.-L. Vay, *Phys. Rev. Letters* **98**, 130405 (2007)
- [11] J.-L. Vay, A. Friedman, D. P. Grote, Proc. 9th International Computational Accelerator Physics Conference (ICAP) 2006, Chamonix, France <http://accelconf.web.cern.ch/AccelConf/ICAP06/PAPERS/WEA3MP02.PDF>

Table 1: Parameters used for simplified configuration of LHC at injection.

| | | |
|------------------------------|----------------|---|
| electron cloud density | ρ_e | $10^{10} - 10^{14} \text{ m}^{-3}$ |
| bunch population | N_b | 1.1×10^{11} |
| beta functions | $\beta_{x,y}$ | 66.0, 71.54 m |
| rms bunch length | σ_z | 0.13 m |
| rms beam size | $\sigma_{x,y}$ | 0.884 mm |
| rms momentum spread | δ_{rms} | 0 |
| circumference | C | 26.659 km |
| nominal tunes | $Q_{x,y}$ | 64.28, 59.31 |
| relativistic factor) | γ | 479.6 |
| pipe radius | R_p | 2.2 cm (with flat tops at ± 1.8 cm) |
| initial beam position offset | δx | $0.1 \sigma_x$ |
| initial beam velocity offset | δv_y | $0.1 v_{y,th}$ |

Table 2: Simulation parameters.

| | | |
|---|------------------|--|
| # of macro-electrons | N_e | 65536/slice |
| # of macro-protons | N_p | 3×10^5 |
| transverse size of the grid (Table 3 & 4) | $L_x \times L_y$ | 4.4cm \times 4.4cm |
| transverse size of the grids (Fig. 1) | $L_x \times L_y$ | 4.4cm \times 4.4cm (level 1) 2.2cm \times 2.2cm (level 2) 1.1cm \times 1.1cm (level 3) 5.5mm \times 5.5mm (level 4) 2.75mm \times 2.75mm (level 5) |
| # of grid points | $N_x \times N_y$ | 128 \times 128 16 \times 16 (all levels) |
| bunch/grid extension in z | L_z | $\pm 4 \sigma_z$ |
| # of slices | N_z | 128 |
| # of ecloud stations | N_{stn} | 10-3000 |
| # of turns | N_t | 1 |
| # of processors | N_{proc} | 32 |

Table 3: Fractional RMS emittance change for quasistatic runs (without beam space-charge).

| $N_e (m^{-3})$ | quasistatic maps (QSM) | | quasistatic Leap-Frog (QSL) | |
|----------------|------------------------|-----------------------|-----------------------------|-----------------------|
| | x | y | x | y |
| 10^{10} | -5.50×10^{-8} | 6.35×10^{-8} | -2.35×10^{-7} | 2.00×10^{-7} |
| 10^{11} | -4.66×10^{-7} | 7.41×10^{-7} | -1.73×10^{-6} | 2.65×10^{-6} |
| 10^{12} | -3.44×10^{-6} | 4.20×10^{-5} | 2.79×10^{-5} | 1.01×10^{-4} |
| 10^{13} | 5.34×10^{-5} | 3.00×10^{-4} | 1.92×10^{-3} | 2.27×10^{-3} |
| 10^{14} | 6.75×10^{-2} | 1.45×10^{-1} | 6.72×10^{-2} | 1.35×10^{-1} |

Table 4: Fractional RMS emittance change for quasistatic runs (including beam space-charge).

| $N_e (m^{-3})$ | quasistatic maps (QSM) | | quasistatic Leap-Frog (QSL) | | PIC boosted frame | |
|----------------|------------------------|------------------------|-----------------------------|-----------------------|-----------------------|-----------------------|
| | x | y | x | y | x | y |
| 10^{10} | -1.30×10^{-5} | -1.52×10^{-5} | -7.79×10^{-6} | 8.75×10^{-6} | 5.13×10^{-6} | 9.52×10^{-6} |
| 10^{11} | -1.34×10^{-5} | -1.58×10^{-5} | -9.34×10^{-6} | 1.12×10^{-5} | 6.23×10^{-6} | 9.51×10^{-6} |
| 10^{12} | -1.64×10^{-5} | 2.70×10^{-5} | 2.01×10^{-5} | 1.10×10^{-4} | 2.08×10^{-5} | 2.33×10^{-5} |
| 10^{13} | 4.03×10^{-5} | 3.15×10^{-4} | 1.91×10^{-3} | 2.28×10^{-3} | 1.81×10^{-3} | 2.14×10^{-3} |
| 10^{14} | 6.72×10^{-2} | 1.45×10^{-1} | 6.71×10^{-2} | 1.35×10^{-1} | 7.29×10^{-2} | 2.38×10^{-1} |